NIH-PA Author Manuscript

Cerebral morphology and dopamine D_2/D_3 receptor distribution in humans: A combined [18F]fallypride and voxel-based morphometry study

Neil D. Woodward[1], **David H. Zald**[2], **Zhaohua Ding**[4], **Patrizia Riccardi**, **M. Sib Ansari**[4], **Ronald M. Baldwin**[4], **Ronald L. Cowan**[1], **Rui Li**[3], and **Robert M. Kessler**[3]

[1] Psychiatric Neuroimaging Program, Vanderbilt University School of Medicine, Nashville, TN

[2] Department of Psychology, Vanderbilt University, Nashville, TN

[3] Department of Radiology, Vanderbilt University Medical Center, Nashville, TN

[4] Vanderbilt Institute of Imaging Sciences, Vanderbilt University, Nashville, TN

Abstract

The relationship between cerebral morphology and the expression of dopamine receptors has not been extensively studied in humans. Elucidation of such relationships may have important methodological implications for clinical studies of dopamine receptor ligand binding differences between control and patient groups. The association between cerebral morphology and dopamine receptor distribution was examined in 45 healthy subjects who completed T1-weighted structural MRI and PET scanning with the D_2/D_3 ligand [18F]fallypride. Optimized voxel-based morphometry was used to create grey matter volume and density images. Grey matter volume and density images were correlated with binding potential (BP_{ND}) images on a voxel-by-voxel basis using the Biological Parametric Mapping toolbox. Associations between cerebral morphology and BP_{ND} were also examined for selected regions-of-interest (ROIs) after spatial normalization. Voxel-wise analyses indicated that grey matter volume and density positively correlated with BP_{ND} throughout the midbrain, including the substantia nigra. Positive correlations were observed in medial cortical areas, including anterior cingulate and medial prefrontal cortex, and circumscribed regions of the temporal, frontal, and parietal lobes. ROI analyses revealed significant positive correlations between BP_{ND} and cerebral morphology in the caudate, thalamus, and amygdala. Few negative correlations between morphology and BP_{ND} were observed. Overall, grey matter density appeared more strongly correlated with BP_{ND} than grey matter volume. Cerebral morphology, particularly grey matter density, correlates with [18F]fallypride BP_{ND} in a regionally specific manner. Clinical studies comparing dopamine receptor availability between clinical and control groups may benefit by accounting for potential differences in cerebral morphology that exist even after spatial normalization.

Address Correspondence to: Neil D. Woodward Ph.D., Post-Doctoral Research Fellow, Psychiatric Neuroimaging Program, Vanderbilt Psychiatric Hospital, Suite 3057, 1601 23rd Ave. S., Nashville, TN 37212, Phone: 615.322.8361, Fax: 615.936.3563.

Keywords

Positron Emission Tomography; Fallypride; Dopamine D_2/D_3 Receptors; Voxel-based Morphometry

Introduction

Over the past two decades positron emission tomography (PET) imaging of dopamine (DA) receptor levels and structural magnetic resonance imaging (MRI) have dramatically expanded our understanding of psychopathology and other behavioral phenotypes. In the clinical realm for example, PET imaging with DA receptor radioligands and MRI have been instrumental in identifying localized changes in DA receptor expression and brain morphology in schizophrenia and substance abuse disorders (Volkow et al., 2008; Zipursky et al., 2007). Parallel investigations of healthy individuals have provided evidence of associations between DA receptor levels or brain structure and behavioral traits. For example, significant associations between regional DA receptor concentrations and personality traits, and hippocampal volume and spatial memory abilities have been identified (Breier et al., 1998; Kestler et al., 2000; Maguire et al., 2000).

To date, the relationship between brain morphology and DA receptor levels has not been systematically investigated in humans. This is surprising given evidence that DA neurotransmission may influence cerebral morphology during development and adulthood. Disruption or depletion of normal neonatal DA function results in reduced pyramidal cell dendrite length, especially in cortical areas that receive significant DA projections such as the anterior cingulate and prefrontal cortex (PFC) (Jones et al., 1996; Kalsbeek et al., 1989; Wang and Deutch, 2008). Conversely, activation of DA D_2 receptors induces neurite elongation (preferentially axonal) in cortical regions (Reinoso et al., 1996). Evidence that neonatal DA depletion affects the macrostructure of the cortex is mixed with reports of both decreases and no change in cortical thickness; although morphological changes at this level may be subtle and/or restricted to specific cortical layers (Alvarez et al., 2002; Kalsbeek et al., 1987; Kalsbeek et al., 1989; Pappas et al., 1992). Evidence of an association between the DA receptor D4 (DRD4) 7-repeat allele and cortical thickness in normal children and those with attention-deficit/hyperactivity disorder (ADHD) indirectly supports an association between DA receptors and cortical development in humans (Shaw et al., 2007). In adulthood, chronic treatment with DA antagonists, D_2 receptor antagonists in particular, reliably increases the volume of basal ganglia structures, especially the caudate, in both rodents and humans and may also increase the thickness of cortical layer V in non-human primates (Chakos et al., 1994; Lieberman et al., 2005; Selemon et al., 1999). The volume increase in the caudate associated with D_2 antagonism is often attributed to a cascade of effects resulting from post-synaptic antagonism including antipsychotic induced disinhibition of striatal neurons, concomitant hypertrophy, and compensatory up-regulation of D_2 receptors (Benes et al., 1985; Chakos et al., 1994; Joyce, 2001). Interestingly, D_2 antagonism is associated with increased expression of D_2 mRNA in the PFC and temporal cortex, and glial cell proliferation (Selemon et al., 1999). Taken together, these findings suggest that there may be a link between cerebral structure and the expression of DA D_2 receptors, although the mechanisms underlying the association are not fully understood.

Elucidation of the relationship between cerebral morphology and the expression of DA D_2 receptors may have important methodological implications for PET studies. Structural brain information acquired in PET imaging studies is rarely integrated into data analysis, beyond being used for the purposes of spatial normalization or region-of-interest (ROI) definition. Moreover, even when structural data is incorporated into PET imaging analyses it is usually

treated as a nuisance variable (Ito et al., 2008). Spatial normalization and ROI analyses can control for partial volume effects; however, neither method may adequately account for individual differences in brain structure. ROIs can be used to correct for individual differences in neuroanatomy, provided volume estimates derived from the ROIs are included as covariates in statistical analyses of binding potential (BP_{ND}) data, although this is rarely done. It is generally assumed that spatial normalization corrects for overall variability in brain shape that exists across subjects by warping brains to a common stereotactic space. However, spatial normalization does not account for subtle differences in cerebral morphology that remain after spatial normalization. Residual variability in brain structure following spatial normalization is potentially very informative. Indeed, examination of the residual differences in morphology that exist after spatial normalization is central to voxel-based morphometry (VBM) and related morphometric techniques (Ashburner and Friston, 2000; Thompson et al., 2004). Such information is rarely incorporated into PET imaging studies (e.g. Ito et al., 2008). Thus, the extent to which residual differences in cerebral morphology relates to BP_{ND} is unknown.

Failure to appropriately control for brain structure is especially problematic in clinical PET studies if the regions demonstrating changes in receptor expression and grey matter volume overlap. This is perhaps best exemplified by studies of schizophrenia patients. Schizophrenia is characterized by localized grey matter changes in multiple neocortical and sub-cortical regions, including the medial PFC, structures of the temporal lobe, and basal ganglia; areas that express DA receptors at levels high enough to be detected in vivo using available radioligands (Honea et al., 2005; Mukherjee et al., 2005; Shenton et al., 2001). Reduced grey matter volume and DA receptor density in the thalamus has been reported by a number of investigators (Buchsbaum et al., 2006; Kemether et al., 2003). Indeed, in separate studies, Buchsbaum and colleagues reported reduced D_2/D_3 receptor concentration and grey matter volume loss in the dorsomedial and pulvinar sub-nuclei of the thalamus in a sample of 15 neuroleptic naïve patients (Buchsbaum et al., 2006; Kemether et al., 2003). However, the relationship between receptor levels and brain volume was not examined. Consequently, it remains unclear if reduced receptor expression in the thalamus is a primary pathophysiological feature of the disorder or is perhaps secondary to grey matter volume loss.

To better understand the relationship between DA receptor distribution and cerebral morphology, we examined the relationships between brain morphology and DA D_2-like receptor binding in humans. We performed structural MRI and PET imaging of the high affinity D_2-like ligand [^{18}F]fallypride in 45 healthy adults. The relationships between D_2-like BP_{ND} and structural features were examined using voxel-based morphometry with BP_{ND} treated as a covariate of interest on a voxel-by-voxel basis using the Biological Parametric Mapping (BPM) toolbox developed by Casanova and colleagues (Casanova et al., 2007). This approach was supplemented with an examination of BP_{ND} and volume/density for several subcortical regions of interest (ROIs) expressing relatively high levels of D_2-like receptors.

Material and methods

Participants

45 subjects, 24 men and 21 women, mean age=24.4 (SD=5.8), with no history of psychiatric illness were recruited to participate through advertisements and word-of-mouth. All subjects were right-hand dominant and non-smokers. Exclusion criteria included history of neurological or psychiatric disorder, severe past or concomitant medical illness, borderline elevated blood pressure, any psychotropic medication usage over the preceding 6 months, history of substance abuse or dependence, inability to provide written informed consent, and pregnancy or lactation. All subjects received a physical and neurological examination, blood chemistries, urine analysis and drug screen, EKG, and underwent the Structured Clinical Interview for Diagnosing DSM-IV Disorders (SCID: First et al., 1996), to rule out Axis I psychopathology.

This study was approved by the Vanderbilt University Institutional Review Board. Informed consent was obtained in writing from each subject following a thorough description of the experimental procedure, including benefits and potential risks.

PET scan acquisition and structural imaging

Subjects underwent a PET study which was performed on a GE Discovery LS PET scanner. 3-D emission acquisitions and transmission attenuation correction scans were performed following a 5.0mCi slow bolus injection of $[^{18}F]$ fallypride (specific activity greater than 3000Ci/mmol). Serial scans started simultaneously with the bolus injection of $[^{18}F]$fallypride and were obtained for approximately 3.5h. The initial scan sequence coincided with the start of the $[^{18}F]$fallypride injection and included the following frames: 8 for 15s, 6 for 30 s, 5 for 1 min, 2 for 2.5 min, 3 for 5 min, and 3 for 10 min. After the initial scan sequence, a 10-min transmission scan was obtained and the subject given a break. At approximately 85–90min post-injection, a second scan sequence of two frames of 25min each followed by a second transmission scan was obtained. The subject was then allowed a second scan break, and at approximately 165–170min, a 40-min emission scan followed by a third transmission scan was obtained. Parametric images of DA D_2/D_3 receptor BP_{ND} were calculated on a voxel-by-voxel basis using the full reference region method (Lammertsma et al., 1996), with the cerebellum serving as the reference region.

A high-resolution, T1-weighted sagittal SPGR sequence (TE=3.6 ms, TR=18.9 ms, TI=400 ms, in-plane resolution=0.5×0.5 mm (n=31) or 1.0×1.0 mm (n=14); slice thickness of 1.0–1.4 mm) was obtained on each subject. All structural scans were acquired on the same GE Signa LXi echospeed 1.5 T MRI scanner located at Vanderbilt University Medical Center. Scanning protocol, one of three, was entered as a nuisance covariate in the subsequent statistical analyses.

Consistent with our prior studies, each subject's serial PET scans were coregistered to reduce potential modeling errors due to head motion using a mutual information based rigid body algorithm (Riccardi et al., 2006). Each participants BP_{ND} image was aligned with their target T1-weighted MRI based on the coregistration of the weighted average of the PET dynamic scans to the MRI using a mutual information rigid body algorithm (Maes et al., 1997; Pluim et al., 2000). All subsequent image processing and statistical analysis were performed using the SPM2 package (http://www.fil.ion.ucl.ac.uk/spm). Following coregistration, the structural MRIs were spatially normalized to the MNI152 T1 template brain and the warping parameters derived from normalization were then applied to the coregistered PET image to bring it into stereotactic space. Cerebral grey matter volume and density images were obtained from the original T1-weighted SPGRs using the 'optimized' VBM procedure (Good et al., 2001). Briefly, the images were first centered on the anterior commissure and normalized to the MNI template using a 12-parameter affine registration algorithm. Next, grey matter, white matter, and cerebrospinal fluid (CSF) templates were created by segmenting and spatially normalizing the original images then averaging each tissue class across subjects. Each template image (T1, grey matter, white matter, CSF) was then smoothed with an 8 mm FWHM Gaussian kernel. Following the creation of the template images, the original images underwent iterative segmentation and normalizations steps, first in native space, then in stereotactic space, using the customized, study-specific templates as tissue priors to optimize segmentation. After the final segmentation and normalization steps, the segmented images were multiplied (i.e. modulated) by the voxel-wise Jacobian determinants obtained during spatial normalization, thereby preserving the original volume of the images. Thus, two sets of grey matter images, modulated (i.e. volume) and unmodulated (i.e. density), were created. Finally, the modulated and unmodulated grey matter segmented images were smoothed with an 8 mm FWHM Gaussian kernel. The BP_{ND} images were not smoothed due to the inherent smoothness of these

images which approximated 8 mm in the x, y, and z dimensions. All images (parametric BP_{ND} maps, grey matter density, and grey matter volume) were re-sampled to $2 \times 2 \times 2$ mm voxels.

Statistical analysis

Prior to statistically analyzing the images, masks were created to exclude voxels with low values, either in BP_{ND} or grey matter volume/density. The resultant masks excluded voxels with BP_{ND} or grey matter volume/density below 0.15. Correlations between fallypride BP_{ND} and grey matter volume or density were examined on a voxel-by-voxel basis using the Biological Parametric Mapping (BPM) toolbox (Casanova et al., 2007). The BPM toolbox examines correlations between multi-modal images co-registered and aligned within the same space (i.e. MNI space). Statistical parametric maps displaying the voxel-wise partial correlation between fallypride BP_{ND} and grey matter volume or density were calculating after covarying for age, gender, structural scanning parameters, and, for the grey matter volume analysis, global grey matter volume. As recommended by the authors of the BPM toolbox, the resultant statistical parametric maps were calculated as non-homologous correlation maps and corrected for multiple comparisons at the cluster corrected alpha=.05 for a voxel-wise threshold of p<.001. Significant clusters were converted from MNI coordinates to Talairach coordinates using the ICBM_SPM2Tal transformation created by Lancaster and colleagues (Lancaster et al., 2007).

Neuroreceptor mapping studies often utilize ROI analyses instead, or in addition, to voxel-wise analyses. However, ROI analyses may also be impacted by differences in grey matter characteristics. Consequently, in addition to being relevant to voxel-wise analysis, significant associations between morphology and BP_{ND} at the ROI level may have implications for PET imaging studies employing an ROI approach. To determine if morphology-BP_{ND} associations might impact ROI analyses, BP_{ND}, grey matter volume, and grey matter density were extracted from the left and right caudate, putamen, thalamus, amygdala, and hippocampus, and correlations between the morphological measures and BP_{ND} were performed for each ROI. These subcortical ROIs were selected because they represent the greatest targets of midbrain DA projections, have significant D_2/D_3 receptor levels, and are frequently the focus of neuroreceptor mapping studies examining group differences in DA D_2/D_3 levels (Mukherjee et al., 2002; Riccardi et al., 2005). Mean BP_{ND}, grey matter density, and volume were extracted from the ROIs using the ExtractVals toolbox (http://www.fil.ion.ucl.ac.uk/spm/ext/#ExtractVals). The caudate, putamen, and thalamus ROIs were derived from the International Consortium for Brain Mapping (ICBM) probabilistic atlas (Shattuck et al., 2008). The hippocampus and amygdala ROIs were created using the Wake Forrest University Pick Atlas (Maldjian et al., 2003) and smoothed with an 8 mm kernel to account for anatomical variation in subjects that exists even after normalization. Correlations between grey matter volume and BP_{ND} were calculated as partial correlations after correcting for global grey matter volume.

Results

Voxelwise analysis

Grey matter volume correlations with binding potential—Areas of the brain where grey matter volume and BP_{ND} were correlated at the corrected alpha level are presented in Table 1 and Figure 1. Volume and BP_{ND} were correlated in a large region of the brainstem that extended from the superior aspect of the pons to the ventro-medial thalamus. This cluster included prominent peaks of correlation within the red nucleus, substantia nigra (SN), and thalamus that tended to be more widespread on the right side. Smaller clusters of positive correlations between volume and BP_{ND} were observed in regions of the prefrontal cortex

corresponding to Brodmann's areas (BA) 6, 9, and 47, parietal lobe, including inferior parietal lobule (BA 40) and precuneus (BA 7), and temporal lobe. An inverse correlation between volume and BP_{ND} was observed in the right parahippocampal gyrus corresponding to BA 34 and 36. Correlations, in absolute values, ranged from .51 to .73. Thus, grey matter volume accounted for approximately 26–53% of the variance in BP_{ND} within the significant clusters identified.

Grey matter density correlations with binding potential—Areas of the brain where grey matter density and BP_{ND} were correlated after correcting for multiple comparisons are presented in Table 2 and Figure 2. The correlations between grey matter density and BP_{ND} appeared stronger and more widespread than the correlations between grey matter volume and BP_{ND}. Similar to the volumetric analysis, grey matter density and BP_{ND} were correlated in a large region of the midbrain that encompassed the red nucleus and SN, and extended up to the ventro-medial thalamus. As with the volumetric analysis, the correlations tended to be more prominent on the right side of the midbrain. Extensive positive correlations between BP_{ND} and density were observed in midline brain structures including a large cluster in the cingulate that extended from pre-genual BA 32 to approximately BA 23 of the ventral posterior cingulate cortex. Correlations between density and BP_{ND} within the cingulate gyrus appeared more extensive in the left hemisphere. Additional positive correlations were observed in midline structures including medial frontal areas corresponding to BA 6 and BA 8, and BA 7 in the precuneus. Multiple clusters were observed throughout the cortex including prefrontal cortical regions, bilateral insula, superior temporal gyrus, and parietal lobe (see Figure 3). Circumscribed clusters of negative correlation were observed bilaterally in the parahippocampal gyrus and right inferior frontal cortex corresponding to BA 47. The magnitude of the correlations ranged from .48 to .77 indicating that grey matter density explained 23–60% of the variance in BP_{ND} within the clusters indentified in the whole brain analysis.

Grey matter segmentation results in midbrain and basal ganglia—The validity of the results reported in the voxel-wise analyses rests upon the quality of the grey matter segmented images derived from VBM. As such, selected slices of the grey matter segmented images and corresponding normalized T1 images for three subjects at the level of the midbrain and basal ganglia are presented in Supplemental Figure 1.

Region-of-interest analysis—Results from the ROI analysis are presented in Table 3. Both volume and density correlated with BP_{ND} in several ROIs; however, similar to the voxel-wise analysis, density correlated more strongly with BP_{ND} than volume. Grey matter density and BP_{ND} were moderately correlated in bilateral caudate, thalamus, and amygdala (r ranged from .15 to .53). Volume and BP_{ND} were positively correlated in the bilateral caudate (r=.31-.41, p<.05). The amount of variance in BP_{ND} explained by grey matter volume and density ranged from 0% to 23% and 2% to 28%, respectively.

Discussion

The current results indicate that cerebral morphology, operationally defined as grey matter volume and density, correlates with the expression of D_2-like receptors in a regionally specific manner in the human brain. Broadly, the association between morphology and BP_{ND} was strongest in areas of the midbrain, including the substantia nigra, midline cortical areas, including the anterior cingulate and medial PFC, insula, superior temporal gyrus, and circumscribed regions of the frontal and parietal lobes. Complementary ROI analyses revealed additional correlations in the caudate, thalamus, and amygdala. There are at least two possible explanations for the observed associations. The most straightforward interpretation is that grey matter positively correlates with D_2 receptors simply because the denser or larger the volume

of grey matter, the more D_2 receptors it can support. In cortex this presumably relates to post-synaptic receptor expression, whereas in the midbrain it probably reflects presynaptic expression of somatodendritic autoreceptors. An alternative explanation is that the expression of DA D_2-like receptors, and by extension DA function, alters cerebral structure during development and/or adulthood. As briefly reviewed earlier, disruption of DA function leads to changes at the neuronal (i.e. dendritic length) and macrostructural (i.e. cortical thickness) levels of cerebral morphology (Alvarez et al., 2002; Jones et al., 1996; Kalsbeek et al., 1987; Kalsbeek et al., 1989; Pappas et al., 1992; Reinoso et al., 1996; Wang and Deutch, 2008). The regional specificity of the associations and the presence of inverse correlations in some regions support the latter hypothesis. Examination of the associations between other in vivo markers of DA function, including pre and post synaptic radiotracers such as $[^{18}F]DOPA$ and $[^{11}C]NNC$-112, and cerebral morphology would help to determine the specificity of the current findings and elucidate the mechanisms underlying the associations. Similarly, simultaneous application of VBM and PET imaging in non-human primates prior to and after manipulation of dopamine functioning would also facilitate interpretation of human studies. Animal studies examining the relationship between grey matter thickness and the relative concentration of dopamine receptors within a specific region would be most beneficial.

The implications of the current findings are largely methodological until the causal relationship between cerebral morphology and the expression of DA receptors is better understood in non-human primates and humans. The current findings strongly suggest that PET imaging studies of $[^{18}F]fallypride$, and possibly other dopamine receptor ligands, may benefit by more fully integrating individual differences in cerebral morphology into data analyses. The current results are particularly pertinent to whole brain voxel-wise analyses. As mentioned in the introduction, it is common practice to warp BP_{ND} images to a standard template brain (i.e. Talairach or MNI space) prior to performing statistical analyses. The assumption underlying this method is that spatial normalization corrects for individual differences in cerebral morphology allowing for direct examination of voxel-wise BP_{ND}. The current results suggest that this method may be improved upon. Spatial normalization, as implemented in the SPM package, does not perfectly warp brains to a template. Rather, the goal is to correct for global shape differences across individuals (Ashburner and Friston, 2000). Residual differences in neuroanatomy after spatial normalization underlies VBM and comparison of these differences between groups has provided compelling evidence for structural brain changes, beyond those identified using traditional manual tracing techniques, in psychiatric and neurological disorders (Honea et al., 2005; Keller and Roberts, 2008). The current findings indicate that individual differences in cerebral morphology that remain after spatial normalization correlates with dopamine D_2-like receptor BP_{ND}. The implications of the findings are further underscored by the fact that the correlations between cerebral morphology and BP_{ND} were most prominent in cortical regions demonstrating the highest $[^{18}F]fallypride$ BP_{ND}, including the anterior cingulate, medial PFC, and regions of the temporal cortex (Mukherjee et al., 2002). The results suggest that the statistical power of between groups or association studies may be improved by including grey matter density as a covariate in statistical analyses to remove unwanted variance in BP_{ND} related to individual differences in cerebral morphology. For a practical implication of the current results, consider the following example. In the current sample, females demonstrated significantly greater BP_{ND} than males in the caudate and hippocampus ROIs (all independent groups t-test p-values<.05). However, only the gender effect observed for the hippocampus ROI remained significant after covarying for grey matter density (main effect of gender p<.05 for left and right hippocampus for univariate ANCOVA). Consequently, the gender differences in BP_{ND} observed in the caudate appear to be driven by cerebral morphology differences between men and women, whereas the greater BP_{ND} observed in the hippocampus in women is independent of cerebral morphology.

There are few prior studies to compare the present results to and we are not aware of any other study examining correlations between cerebral morphology and [^{18}F]fallypride BP_{ND} on a voxel-wise basis. Nonetheless, the current results are consistent with an earlier study that also did not find a correlation between hippocampal ROI volume and [^{18}F]fallypride BP_{ND} in a small group of patients with medial temporal lobe epilepsy and healthy comparison subjects (Werhahn et al., 2006). The apparent specificity of the correlations between BP_{ND} and volume/ density is noteworthy, particularly for sub-cortical structures that demonstrate the highest levels of [^{18}F]fallypride BP_{ND}. ROI analyses revealed significant associations between grey matter volume/density and [^{18}F]fallypride BP_{ND} in the caudate, but not putamen. It is possible that the absence of a significant relationship between receptor concentration and grey matter volume/density in the putamen is due to the relatively poorer grey/white matter contrast observed in the putamen relative to the caudate. Reduced grey/white contrast can adversely affect the sensitivity of automated segmentation algorithms used in VBM thereby reducing the chances of detecting a significant relationship in this region (Douaud et al., 2006). However, several observations suggest that the apparent lack of association between cerebral morphology and BP_{ND} in the putamen was not due to poor grey/white matter contrast in central brain structures. First, the potentially poorer grey/white contrast in central brain structures did not appear to hamper the ability to detect a significant relationship between grey matter density and BP_{ND} in the thalamus, a region notoriously difficult to segment on MRIs (Shenton et al., 2001). Second, the quality of the segmentation of the basal ganglia appeared reasonable upon visual inspection, at least for the caudate and putamen (see Supplemental Figure 1). The validity of the correlations identified in the midbrain, substantia nigra in particular, also rest upon the quality of the segmentation in this region. Numerous VBM studies have identified significant findings in the midbrain and inspection of the segmentation results for the present study confirmed that VBM is sensitive to grey/white matter differences in the region. However, replication using proton density scans, which provide better delineation of the substantia nigra than standard T1 weighted sequences, would increase confidence in the current findings.

The pattern of correlations with BP_{ND} was similar for both volume and density; however, the latter were greater in magnitude and more extensive for both the voxelwise and ROI analyses. It is unclear why the relationship between density and BP_{ND} appeared stronger than the associations between BP_{ND} and volume. Density and volume measures derived from VBM represent separate, but complementary aspects of cerebral morphology. Density is the relative amount of grey matter within a voxel after spatial normalization, whereas volume reflects the relative concentration after adjusting (i.e. modulating) voxel intensity values for the morphometric changes introduced during spatial normalization (Ashburner and Friston, 2000). It is possible that the closer association observed between density and BP_{ND} was due to the fact that neither image is modulated to incorporate information contained in the deformation fields derived from spatial normalization. In contrast, the voxel values in the volume images are modulated to retain information about the original morphometry of individual brains prior to spatial normalization. The relationships between BP_{ND} and volume might have been just as robust had the normalized BP_{ND} images also been modified to reflect information contained in the images prior to spatial normalization. In addition, a recent large scale VBM study comparing patients with schizophrenia to controls found that the standard error of measurement was larger for volume than density indicating that the latter has greater power to detect significant associations (Meda et al., 2008). It is also worth reiterating that global grey matter volume served as an additional covariate to the volume- BP_{ND} correlation analysis resulting in a slight diminution of statistical power compared to the grey matter density/BP_{ND} correlation analysis.

Positive associations between volume/density and BP_{ND} are not unexpected since it is reasonable to hypothesize that BP_{ND} in a region expressing DA receptors will vary positively with the size or relative density of grey matter within the region. Negative correlations on the

other hand are unexpected. Consistent inverse associations between BP$_{ND}$ and cerebral morphology were observed in circumscribed regions of the hippocampus and ventral hippocampal/parahippocampal region. The hippocampus and parahippocampal region receives dense DA projections from midbrain nuclei and dopaminergic drugs can modulate synaptic activity and plasticity in this region. Specifically, increasing DA activity in this area reduces neuronal firing and suppresses synaptic plasticity (Caruana et al., 2007; Caruana and Chapman, 2008). Longitudinal studies have established that VBM is sensitive to learning induced changes in synaptic plasticity suggesting that VBM is sensitive to the fine microstructure of the brain (Ilg et al., 2008). Speculatively, reduced dopamine activity in this region, as evinced by fewer DA receptors, may result in increased grey matter density. Alternatively, or perhaps in conjunction, the inverse association in this region might also relate to glial cell proliferation in response to reduced DA activity. Future research will be necessary to confirm this finding and clarify the causal direction and consequences of the association between DA functioning and hippocampal/parahippocampal structure.

Supplementary Material

Refer to Web version on PubMed Central for supplementary material.

Acknowledgments

References

Alvarez C, Vitalis T, Fon EA, Hanoun N, Hamon M, Seif I, Edwards R, Gaspar P, Cases O. Effects of genetic depletion of monoamines on somatosensory cortical development. Neuroscience 2002;115:753–764. [PubMed: 12435414]

Ashburner J, Friston KJ. Voxel-based morphometry--the methods. Neuroimage 2000;11:805–821. [PubMed: 10860804]

Benes FM, Paskevich PA, Davidson J, Domesick VB. The effects of haloperidol on synaptic patterns in the rat striatum. Brain Res 1985;329:265–273. [PubMed: 3978446]

Breier A, Kestler L, Adler C, Elman I, Wiesenfeld N, Malhotra A, Pickar D. Dopamine D2 receptor density and personal detachment in healthy subjects. Am J Psychiatry 1998;155:1440–1442. [PubMed: 9766779]

Buchsbaum MS, Christian BT, Lehrer DS, Narayanan TK, Shi B, Mantil J, Kemether E, Oakes TR, Mukherjee J. D2/D3 dopamine receptor binding with [F-18]fallypride in thalamus and cortex of patients with schizophrenia. Schizophr Res 2006;85:232–244. [PubMed: 16713185]

Caruana DA, Chapman CA. Dopaminergic suppression of synaptic transmission in the lateral entorhinal cortex. Neural Plast 2008;2008:203514. [PubMed: 18769495]

Caruana DA, Reed SJ, Sliz DJ, Chapman CA. Inhibiting dopamine reuptake blocks the induction of long-term potentiation and depression in the lateral entorhinal cortex of awake rats. Neurosci Lett 2007;426:6–11. [PubMed: 17869420]

Casanova R, Srikanth R, Baer A, Laurienti PJ, Burdette JH, Hayasaka S, Flowers L, Wood F, Maldjian JA. Biological parametric mapping: A statistical toolbox for multimodality brain image analysis. Neuroimage 2007;34:137–143. [PubMed: 17070709]

Chakos MH, Lieberman JA, Bilder RM, Borenstein M, Lerner G, Bogerts B, Wu H, Kinon B, Ashtari M. Increase in caudate nuclei volumes of first-episode schizophrenic patients taking antipsychotic drugs. Am J Psychiatry 1994;151:1430–1436. [PubMed: 7916539]

Douaud G, Gaura V, Ribeiro MJ, Lethimonnier F, Maroy R, Verny C, Krystkowiak P, Damier P, Bachoud-Levi AC, Hantraye P, Remy P. Distribution of grey matter atrophy in Huntington's disease

patients: a combined ROI-based and voxel-based morphometric study. Neuroimage 2006;32:1562–1575. [PubMed: 16875847]

First, MB.; Spitzer, RL.; Gibbon, M.; Williams, JBW. Structured Clinical Interview for DSM-IV Axis I Disorders, Clinical Version (SCID-CV). American Psychiatric Press Inc; Washington, D.C: 1996.

Good CD, Johnsrude IS, Ashburner J, Henson RN, Friston KJ, Frackowiak RS. A voxel-based morphometric study of ageing in 465 normal adult human brains. Neuroimage 2001;14:21–36. [PubMed: 11525331]

Honea R, Crow TJ, Passingham D, Mackay CE. Regional deficits in brain volume in schizophrenia: a meta-analysis of voxel-based morphometry studies. Am J Psychiatry 2005;162:2233–2245. [PubMed: 16330585]

Ilg R, Wohlschlager AM, Gaser C, Liebau Y, Dauner R, Woller A, Zimmer C, Zihl J, Muhlau M. Gray matter increase induced by practice correlates with task-specific activation: a combined functional and morphometric magnetic resonance imaging study. J Neurosci 2008;28:4210–4215. [PubMed: 18417700]

Ito H, Takahashi H, Arakawa R, Takano H, Suhara T. Normal database of dopaminergic neurotransmission system in human brain measured by positron emission tomography. Neuroimage 2008;39:555–565. [PubMed: 17962043]

Jones L, Fischer I, Levitt P. Nonuniform alteration of dendritic development in the cerebral cortex following prenatal cocaine exposure. Cereb Cortex 1996;6:431–445. [PubMed: 8670669]

Joyce JN. D2 but not D3 receptors are elevated after 9 or 11 months chronic haloperidol treatment: influence of withdrawal period. Synapse 2001;40:137–144. [PubMed: 11252025]

Kalsbeek A, Buijs RM, Hofman MA, Matthijssen MA, Pool CW, Uylings HB. Effects of neonatal thermal lesioning of the mesocortical dopaminergic projection on the development of the rat prefrontal cortex. Brain Res 1987;429:123–132. [PubMed: 3032369]

Kalsbeek A, Matthijssen MA, Uylings HB. Morphometric analysis of prefrontal cortical development following neonatal lesioning of the dopaminergic mesocortical projection. Exp Brain Res 1989;78:279–289. [PubMed: 2599038]

Keller SS, Roberts N. Voxel-based morphometry of temporal lobe epilepsy: an introduction and review of the literature. Epilepsia 2008;49:741–757. [PubMed: 18177358]

Kemether EM, Buchsbaum MS, Byne W, Hazlett EA, Haznedar M, Brickman AM, Platholi J, Bloom R. Magnetic resonance imaging of mediodorsal, pulvinar, and centromedian nuclei of the thalamus in patients with schizophrenia. Arch Gen Psychiatry 2003;60:983–991. [PubMed: 14557143]

Kestler LP, Malhotra AK, Finch C, Adler C, Breier A. The relation between dopamine D2 receptor density and personality: preliminary evidence from the NEO personality inventory-revised. Neuropsychiatry Neuropsychol Behav Neurol 2000;13:48–52. [PubMed: 10645736]

Lammertsma AA, Bench CJ, Hume SP, Osman S, Gunn K, Brooks DJ, Frackowiak RS. Comparison of methods for analysis of clinical [^{11}C]raclopride studies. J Cereb Blood Flow Metab 1996;16:42–52. [PubMed: 8530554]

Lancaster JL, Tordesillas-Gutierrez D, Martinez M, Salinas F, Evans A, Zilles K, Mazziotta JC, Fox PT. Bias between MNI and Talairach coordinates analyzed using the ICBM-152 brain template. Hum Brain Mapp 2007;28:1194–1205. [PubMed: 17266101]

Lieberman JA, Tollefson GD, Charles C, Zipursky R, Sharma T, Kahn RS, Keefe RS, Green AI, Gur RE, McEvoy J, Perkins D, Hamer RM, Gu H, Tohen M. Antipsychotic drug effects on brain morphology in first-episode psychosis. Arch Gen Psychiatry 2005;62:361–370. [PubMed: 15809403]

Maes F, Collignon A, Vandermeulen D, Marchal G, Suetens P. Multimodality image registration by maximization of mutual information. IEEE Trans Med Imaging 1997;16:187–198. [PubMed: 9101328]

Maguire EA, Gadian DG, Johnsrude IS, Good CD, Ashburner J, Frackowiak RS, Frith CD. Navigation-related structural change in the hippocampi of taxi drivers. Proc Natl Acad Sci USA 2000;97:4398–4403. [PubMed: 10716738]

Maldjian JA, Laurienti PJ, Kraft RA, Burdette JH. An automated method for neuroanatomic and cytoarchitectonic atlas-based interrogation of fMRI data sets. Neuroimage 2003;19:1233–1239. [PubMed: 12880848]

Meda SA, Giuliani NR, Calhoun VD, Jagannathan K, Schretlen DJ, Pulver A, Cascella N, Keshavan M, Kates W, Buchanan R, Sharma T, Pearlson GD. A large scale (N=400) investigation of gray matter differences in schizophrenia using optimized voxel-based morphometry. Schizophr Res 2008;101:95–105. [PubMed: 18378428]

Mukherjee J, Christian BT, Dunigan KA, Shi B, Narayanan TK, Satter M, Mantil J. Brain imaging of 18F-fallypride in normal volunteers: blood analysis, distribution, test-retest studies, and preliminary assessment of sensitivity to aging effects on dopamine D-2/D-3 receptors. Synapse 2002;46:170–188. [PubMed: 12325044]

Mukherjee J, Christian BT, Narayanan TK, Shi B, Collins D. Measurement of d-amphetamine-induced effects on the binding of dopamine D-2/D-3 receptor radioligand, 18F-fallypride in extrastriatal brain regions in non-human primates using PET. Brain Res 2005;1032:77–84. [PubMed: 15680944]

Pappas BA, Murtha SJ, Park GA, Condon KT, Szirtes RM, Laventure SI, Ally A. Neonatal brain dopamine depletion and the cortical and behavioral consequences of enriched postweaning environment. Pharmacol Biochem Behav 1992;42:741–748. [PubMed: 1513856]

Pluim JP, Maintz JB, Viergever MA. Image registration by maximization of combined mutual information and gradient information. IEEE Trans Med Imaging 2000;19:809–814. [PubMed: 11055805]

Reinoso BS, Undie AS, Levitt P. Dopamine receptors mediate differential morphological effects on cerebral cortical neurons in vitro. J Neurosci Res 1996;43:439–453. [PubMed: 8699530]

Riccardi P, Li R, Ansari MS, Zald D, Park S, Dawant B, Anderson S, Doop M, Woodward N, Schoenberg E, Schmidt D, Baldwin R, Kessler R. Amphetamine-induced displacement of [18F] fallypride in striatum and extrastriatal regions in humans. Neuropsychopharmacology 2006;31:1016–1026. [PubMed: 16237395]

Riccardi P, Zald DH, Park S, Li R, Ansari MS, Dawant B, Anderson S, Woodward N, Schmidt D, Baldwin R, Kessler RM. Sex differences in amphetamine induced displacement of [18F] fallypride in striatal and extrastriatal regions: A PET study. Am J Psychiatry. 2005

Selemon LD, Lidow MS, Goldman-Rakic PS. Increased volume and glial density in primate prefrontal cortex associated with chronic antipsychotic drug exposure. Biol Psychiatry 1999;46:161–172. [PubMed: 10418690]

Shattuck DW, Mirza M, Adisetiyo V, Hojatkashani C, Salamon G, Narr KL, Poldrack RA, Bilder RM, Toga AW. Construction of a 3D probabilistic atlas of human cortical structures. Neuroimage 2008;39:1064–1080. [PubMed: 18037310]

Shaw P, Gornick M, Lerch J, Addington A, Seal J, Greenstein D, Sharp W, Evans A, Giedd JN, Castellanos FX, Rapoport JL. Polymorphisms of the dopamine D4 receptor, clinical outcome, and cortical structure in attention-deficit/hyperactivity disorder. Arch Gen Psychiatry 2007;64:921–931. [PubMed: 17679637]

Shenton ME, Dickey CC, Frumin M, McCarley RW. A review of MRI findings in schizophrenia. Schizophr Res 2001;49:1–52. [PubMed: 11343862]

Thompson PM, Hayashi KM, Sowell ER, Gogtay N, Giedd JN, Rapoport JL, de Zubicaray GI, Janke AL, Rose SE, Semple J, Doddrell DM, Wang Y, van Erp TG, Cannon TD, Toga AW. Mapping cortical change in Alzheimer's disease, brain development, and schizophrenia. Neuroimage 2004;23 (Suppl 1):S2–18. [PubMed: 15501091]

Volkow ND, Fowler JS, Wang GJ, Baler R, Telang F. Imaging dopamine's role in drug abuse and addiction. Neuropharmacology. 2008

Wang HD, Deutch AY. Dopamine depletion of the prefrontal cortex induces dendritic spine loss: reversal by atypical antipsychotic drug treatment. Neuropsychopharmacology 2008;33:1276–1286. [PubMed: 17687264]

Werhahn KJ, Landvogt C, Klimpe S, Buchholz HG, Yakushev I, Siessmeier T, Muller-Forell W, Piel M, Rosch F, Glaser M, Schreckenberger M, Bartenstein P. Decreased dopamine D2/D3-receptor binding in temporal lobe epilepsy: an [18F]fallypride PET study. Epilepsia 2006;47:1392–1396. [PubMed: 16922886]

Zipursky RB, Meyer JH, Verhoeff NP. PET and SPECT imaging in psychiatric disorders. Can J Psychiatry 2007;52:146–157. [PubMed: 17479522]
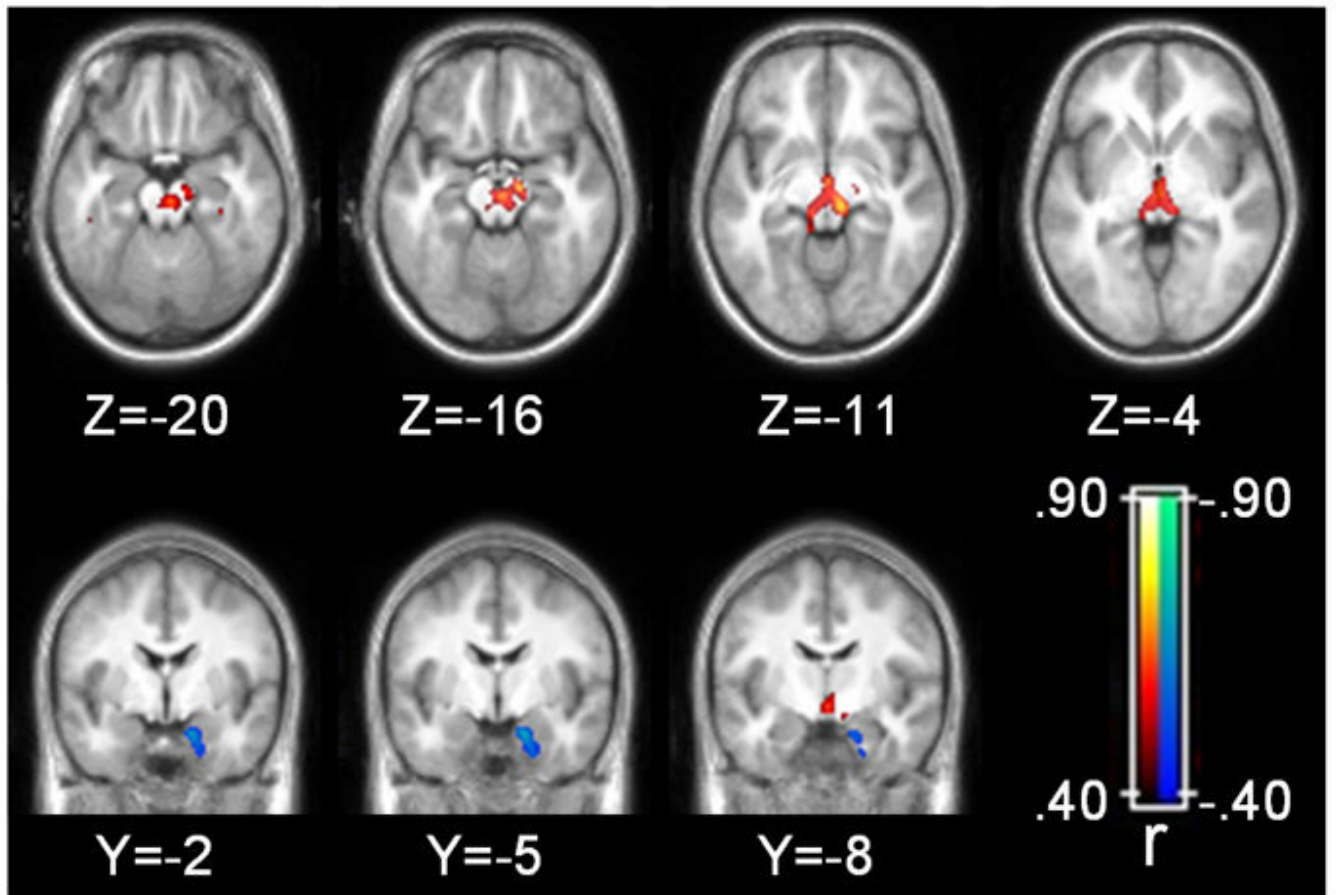
Figure 1.
Grey matter volume correlations with binding potential. Statistical parametric map corrected at whole-brain cluster-wise p<.05. Axial images displayed in neurological format (i.e. left side of brain on left side of image).

Figure 2.
Grey matter density correlations with binding potential. Statistical parametric map corrected at whole-brain cluster-wise p<.05. Axial images displayed in neurological format (i.e. left side of brain on left side of image).

Figure 3.
Grey matter density correlations with binding potential overlaid on a surface rendering of the customized template brain derived from 45 subjects. Statistical parametric map corrected at whole-brain cluster-wise p<.05.
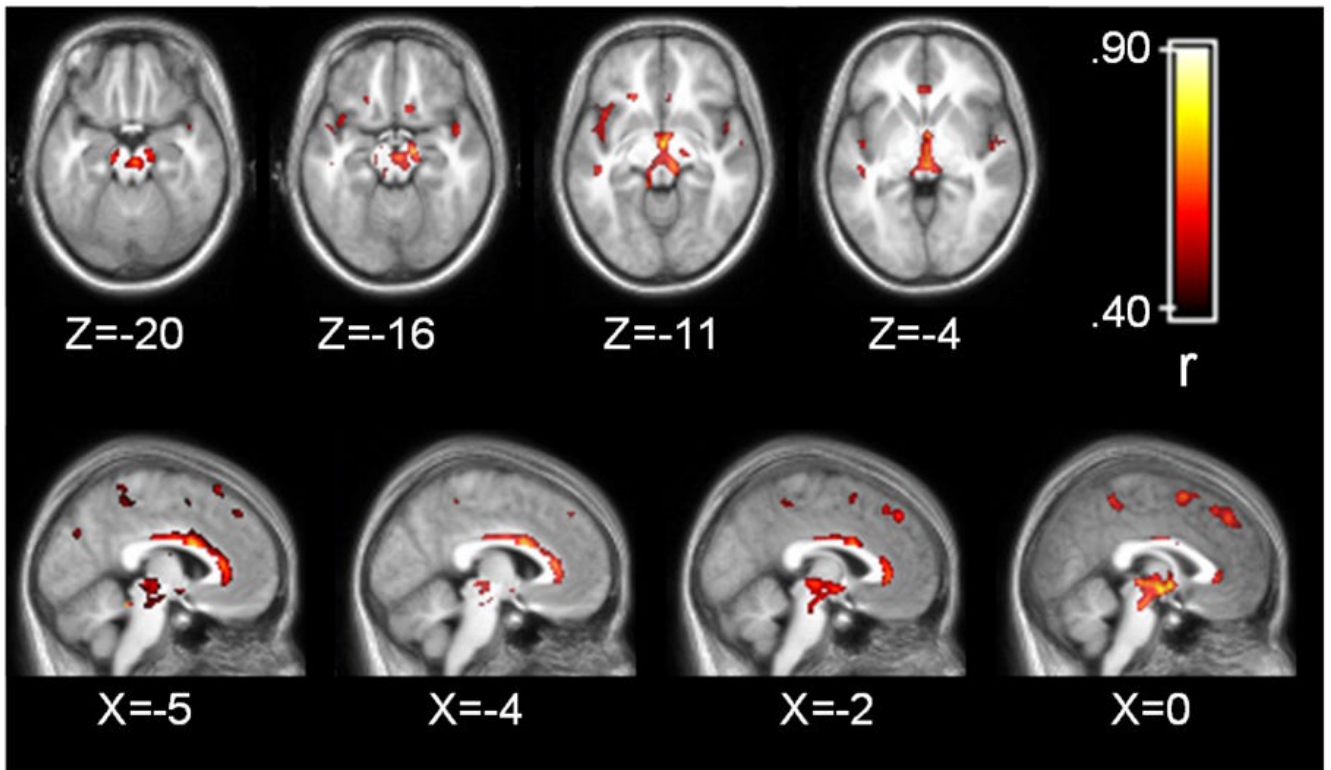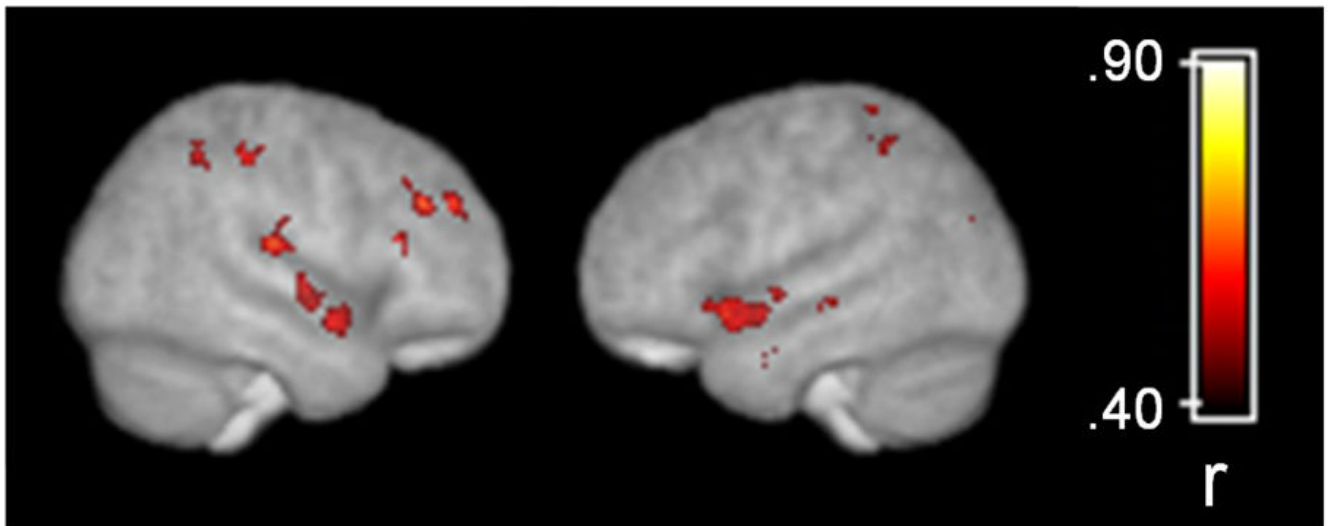
Table 1

Correlations Between [^{18}F]Fallypride BP$_{ND}$ and Grey Matter Volume

		Talairach Coordinates					
	Brain Region	**X**	**Y**	**Z**	**Correlation Coefficient**	**Corrected p-value**	**Voxels***
Positive Correlation	Right Midbrain: Red Nucleus	6	−23	−7	0.73	<.001	693
	Right Midbrain: Substania Nigra	10	−12	−11	0.72		
	Right Thalamus	1	−12	−2	0.69		
	Left Middle Frontal Gyrus (BA 6)	−33	13	43	0.64	.003	72
	Left Middle Frontal Gyrus (BA 6)	−35	7	48	0.57		
	Left Parahippocampal Gyrus (BA 36)	−38	−29	−23	0.60	.008	62
	Left Inferior Temporal Gyrus (BA 20)	−40	−25	−29	0.59		
	Left Inferior Frontal Gyrus (BA 9)	−33	8	24	0.59	.009	61
	Left Middle Frontal Gyrus (BA 9)	−35	17	25	0.52		
	Left Precuneus (BA 31)	−24	−71	24	0.58	.039	46
	Left Inferior Parietal Lobule (BA 40)	−35	−43	43	0.58	.043	45
	Left Precuneus (BA 7)	−28	−47	48	0.51		
	Right Parahippocampal Gyrus (BA 36)	38	−28	−21	0.57	.032	48
	Right Parahippocampal Gyrus (BA 36)	29	−26	−16	0.54		
Negative Correlation	Right Uncus (BA 34)	14	−3	−19	0.71	<.001	143
	Right Uncus (BA 36)	20	−4	−28	0.59		

Table shows up to 3 local maxima within a cluster more than 8.0mm apart

*Voxel size = 2 × 2 × 2 mm

Abbreviations: BA=Brodmann's Area

Table 2

Correlations Between [^{18}F]Fallypride BP$_{ND}$ and Grey Matter Density

	Brain Region	Talairach Coordinates			Correlation Coefficient	Corrected p-value	Voxels[*]
		X	Y	Z			
Positive Correlation	Right Brainstem: Mammillary Body	1	−8	−6	0.77	<.001	844
	Right Brainstem: Substania Nigra	10	−12	−11	0.71		
	Right Brainstem: Red Nucleus	1	−22	−1	0.70		
	Left Cingulate Gyrus (BA 24)	−5	3	28	0.72	<.001	708
	Left Anterior Cingulate (BA 24)	−5	26	14	0.68		
	Left Anterior Cingulate (BA 24)	−1	30	7	0.67		
	Right Caudate Tail	19	−26	20	0.67	<.001	69
	Right Thalamus	23	−27	11	0.60		
	Right Caudate Tail	19	−35	12	0.51		
	Right Middle Frontal Gyrus (BA 9)	32	31	37	0.66	.003	49
	Right Middle Frontal Gyrus (BA 8)	32	24	43	0.52		
	Right Superior Frontal Gyrus (BA 9)	15	38	35	0.66	.001	61
	Right Superior Frontal Gyrus (BA 9)	19	46	32	0.48		
	Left Medial Frontal Gyrus (BA 6)	0	2	57	0.66	<.001	96
	Left Inferior Frontal Gyrus (BA 47)	−19	24	−5	0.64	.014	38
	Left Superior Frontal Gyrus (BA 8)	−2	24	50	0.64	<.001	147
	Left Superior Frontal Gyrus (BA 8)	−1	32	45	0.64		
	Right Postcentral Gyrus (BA 40)	54	−24	17	0.64	<.001	75
	Right Postcentral Gyrus (BA 2)	54	−21	27	0.51		
	Left Superior Temporal Gyrus (BA 22)	−44	−25	−4	0.63	<.001	65
	Left Parahippocampal Gyrus (BA 36)	−43	−21	−13	0.48		
	Right Cingulate Gyrus (BA 24)	12	12	31	0.62	.001	55
	Right Anterior Cingulate (BA 32)	10	25	21	0.60		
	Left Insula (BA 13)	−38	13	−6	0.61	<.001	195
	Left Insula (BA 13)	−42	−9	−1	0.58		
	Left Insula (BA 13)	−40	5	−7	0.57		
	Left Precuneus (BA 7)	−31	−45	45	0.61	<.001	130
	Left Superior Parietal Lobule (BA 7)	−28	−55	51	0.56		

Brain Region	Talairach Coordinates			Correlation Coefficient	Corrected p-value	Voxels[*]
	X	Y	Z			
Left Precuneus (BA 7)	0	−46	49	0.61	<.001	89
Right Precuneus (BA 7)	4	−55	53	0.51		
Left Precuneus (BA 31)	−24	−71	24	0.60	<.001	82
Left Middle Occipital Gyrus (BA 19)	−26	−82	19	0.49		
Left Parahippocampal Gyrus (BA 37)	−14	−17	−16	0.60	.009	41
Right Middle Frontal Gyrus (BA 46)	34	23	21	0.60	.007	43
Right Middle Frontal Gyrus (BA 46)	30	13	24	0.51		
Right Insula (BA 13)	40	1	−9	0.59	.001	57
Right Inferior Parietal Lobule (BA 40)	45	−36	47	0.58	.043	31
Right Insula (BA 13)	40	−17	7	0.57	<.001	68
Right Insula (BA 13)	43	−11	4	0.56		
Right Superior Temporal Gyrus (BA 22)	53	−7	−3	0.54		
Right Inferior Parietal Lobule (BA 40)	39	−55	47	0.56	.043	31
Right Superior Parietal Lobule (BA 7)	30	−55	50	0.51		
Left Fusiform Gyrus (BA 20)	−38	−5	−22	0.56	.031	33
Left Superior Parietal Lobule (BA 7)	−32	−49	62	0.55	.017	37
Left Inferior Parietal Lobule (BA 40)	−41	−50	57	0.51		
Negative Correlation						
Right Uncus (BA 28)	14	−3	−25	0.62	.019	36
Right Inferior Frontal Gyrus (BA 47)	22	11	−21	0.61	.017	37
Left Hippocampus	−28	−11	−13	0.59	.023	35

Table shows up to 3 local maxima more than 8.0mm apart

[*] Voxel size = 2 × 2 × 2 mm

Abbreviations: BA=Brodmann's Area

Table 3

Correlations Between $[^{18}F]$Fallypride BP_{ND} and Grey Matter Volume/Density for Selected Regions of Interest

	Region of Interest										
	Caudate		Putamen		Thalamus		Amygdala		Hippocampus	
	Left	Right	Left	Right	Left	Right	Left	Right	Left	Right
Volume[†]	.41 **	.31 *	−.07	−.22	−.24	−.11	.12	−.09	.01	−.09
Density	.53 **	.52 **	.15	.15	.31 *	.40 **	.33 *	.33 *	.17	.26

[†]Partial correlation after covarying for global grey matter volume

*
p<.05

**
p<.005